Analytical Methods

PAPER

View Article Online
View Journal | View Issue

Cite this: *Anal. Methods*, 2017, **9**, 4726

A sensitive colorimetric aptasensor with a triple-helix molecular switch based on peroxidase-like activity of a DNAzyme for ATP detection

Kosar Shahsavar,[a] Morteza Hosseini, *[ab] Ehsan Shokri,[a] Mohammad Reza Ganjali[cd] and Huangxian Ju[e]

Received 3rd June 2017
Accepted 18th July 2017

DOI: 10.1039/c7ay01381g

rsc.li/methods

A DNAzyme-based colorimetric aptasensor has been fabricated for fast readout and facile detection of adenosine triphosphate (ATP). The sensor consists of an ATP-specific aptamer flanked with cytosine-rich arms at both ends (5′ & 3′) and a peroxidase mimicking DNAzyme which were complexed together to form a functional triple-helix molecular switch (THMS). The DNAzyme strand serves as a signal transduction probe (STP) in the molecular switch. In the presence of ATP, the aptamer binds to it and the THMS complex disassembles. Subsequently the released DNAzyme sequence can form a catalytic G-quadruplex DNAzyme leading to obvious color change. This sensor provides an efficient and stable diagnostic system whilst conserving the inherent catalytic activity of the DNAzyme and the selectivity of the aptamer. The aptasensor response was linear for ATP concentration between 5 and 230 nM (R^2 = 0.9854) with a detection limit of 2.4 nM (S/N = 3). Besides, ATP can be detected in human serum samples with satisfactory results, which demonstrates the potential applications for real analysis.

1 Introduction

Adenosine triphosphate (ATP) is one of the most important compounds in living organisms which works as an energy currency unit within cells.[1] It plays a significant role in the regulation of cellular metabolism and many enzymatic reactions.[2] Also ATP is considered as an indicator for cell viability and cell injury.[3] It has been shown that changes in the ATP level are associated with certain diseases such as angiocardiopathy, Parkinson's and Alzheimer's.[4] Besides this, ATP is used as an index for biomass determinations in clinical microbiology and food quality control analysis.[5]

Thus far, a number of methods have been developed for ATP detection such as electrochemical luminescence,[6,7] chemiluminescence resonance energy transfer strategy,[8] fluorescence spectrophotometry[9] and fluorescence resonance energy transfer.[10] Generally these methods are limited by laborious and expensive labelling and time-consuming processes. Thus, it is necessary to develop a new approach that could improve the simplicity and sensitivity of detection and also reduce the total cost.

DNAzymes (deoxyribozymes) are enzymatically active nucleic acids, which are identified through *in vitro* selection experiments.[11] It is well-known that DNAzymes can catalyze numerous biochemical reactions, including the cleavage of DNA or RNA,[12,13] metalation of porphyrin rings,[14] DNA self-modification and ligation.[15,16] One of the most studied DNAzymes is the hemin/G-quadruplex which can associate with a cofactor, hemin, to form a catalytic DNAzyme.[17] G-quadruplex–hemin complexes with peroxidase-like catalytic activity can catalyze H_2O_2-mediated oxidation of 2,2′-azinobis(3-ethylbenzthiazoline-6-sulfonic acid) diammonium salt (ABTS–H_2O_2 system)[17,18] or 3,3,5,5-tetramethylbenzidine sulfate (TMB) to produce detectable color change.[19]

DNAzymes exhibit several advantages in comparison with protein enzymes such as high thermal stability, low cost, simple synthesis and ease of modification.[20–22] With these obvious advantages, a G-quadruplex DNAzyme has been employed to develop many colorimetric biosensors for the specific and sensitive detection of various targets such as small molecules,[23,24] DNAs[25,26] and proteins.[27,28]

Colorimetric assay is a common method in analytical applications due to its outstanding advantages such as simplicity, low cost, high sensitivity and easiness in signal readout by the naked eye without requiring analytical instruments. Furthermore, colorimetric detection of ATP allows us to analyze the amount of ATP consumption and production for on-site and real-time detection.[29]

[a]*Department of Life Science Engineering, Faculty of New Sciences & Technologies, University of Tehran, Tehran, Iran. E-mail: smhosseini@khayam.ut.ac.ir*

[b]*Medical Biomaterials Research Center, Tehran University of Medical Sciences, Tehran, Iran*

[c]*Center of Excellence in Electrochemistry, Faculty of Chemistry, University of Tehran, Tehran, Iran*

[d]*Biosensor Research Center, Endocrinology & Metabolism Molecular-Cellular Sciences Institute, Tehran University of Medical Sciences, Tehran, Iran*

[e]*State Key Laboratory of Analytical Chemistry for Life Science, Department of Chemistry, Nanjing University, Nanjing 210093, China*

In this study a novel colorimetric aptasensor was developed for detection of ATP *via* a triple-helix molecular switch (THMS) system. The THMS system is generally composed of a label-free target-specific aptamer with two arm segments and a dual-labeled oligonucleotide as a signal transduction probe (STP).[30] In this work for the first time, a new label-free STP was proposed. The G-rich sequence which is used as the STP, is capable of forming a G-quadruplex DNAzyme in the presence of hemin. Compared to molecular beacon-based signalling aptamers and known double-helix DNA molecular switches, the THMS shows distinct advantages, such as high stability and sensitivity while preserving the affinity and specificity of the original aptamer.

2 Materials and methods

The sequence of a DNAzyme (STP) and ATP-binding aptamer (ATP–Apt) flanked with similar arms (CCCTCCC) at both ends was purchased from Shanghai Generay Biotech Co (Table 1). The stock solutions of oligonucleotide probes were prepared with TE buffer and kept frozen until use.

Triton X-100, tetramethylbenzidine (TMB), adenosine triphosphate (ATP), 4-(2-hydroxyethyl)piperazine-1-ethanesulfonic acid sodium salt (HEPES), and hemin were purchased from Sigma-Aldrich Chemical Co. Other chemicals were of analytical grade and were used without further purification.

The stock solution of 1 mg per mL hemin was prepared in dimethyl sulfoxide (DMSO) and stored in darkness at −20 °C. Hemin solutions were diluted to required concentrations in the HEPES buffer (25 mM HEPES, 20 mM KCl, 200 mM NaCl, 0.025% (w/v) Triton X-100, 1% (v/v) DMSO and pH 7.4) prior to use. The human serum samples were supplied by Tehran's Imam Khomeini Hospital.

2.1 Preparation of the triple-helix molecular switch

To prepare the THMS structure, a solution of ATP–Apt and DNAzyme in a binding buffer consisting of 10 mM sodium hydrogen phosphate-citric acid, 300 mM NaCl, and 2.5 mM $MgCl_2$ at pH 4.5 was used. The solution mixture was heated to 88 °C for 10 min in order to dissociate any inter or intra-molecular interactions and then cooled naturally to room temperature and incubated for 2 h. In order to confirm the formation of the THMS, we read the complex absorption alone in the presence of ATP. We also loaded 10 μL of ATP–Apt, STP and THMS solutions in separate lines on agarose gel (3%) and visualized under UV after staining with ethidium bromide. Electrophoresis was performed in 1X TBE buffer at 80 V and room temperature for 30 min.

2.2 Optimizing STP and hemin concentrations

To obtain the optimum concentration of the STP, increasing concentrations of the STP (0–160 nM) were added to 115 nM ATP–Apt (final volume of reaction buffer 90 μL). Mixtures were stored for 2 h at room temperature, and then a constant level of the target and hemin was added to each well. After 1 h incubation, TMB and H_2O_2 were added and the absorbance value was recorded at 450 nm by using a spectrophotometer. For hemin optimization, a range of hemin concentrations (0–130 nM) was added to the STP with a final concentration of 80 nM. Mixtures were incubated for 60 min at room temperature. Absorbance was recorded after addition of TMB and H_2O_2.

2.3 Effect of pH on the formation of the THMS

The formation of the THMS over the range of different pH values (2.5–8.0) in the presence of the STP (80 nM) and ATP–Apt (115 nM) was studied. After 2 h incubation, ATP was added; the reactions were maintained at RT. After incubation with hemin (88 nM), the maximum absorbance of each well was recorded.

2.4 ATP assay (sensitivity and selectivity)

To evaluate the sensitivity of the DNAzyme aptasensor, different concentrations of ATP were added to the THMS solution (0–230 nM) and incubated for 30 min. Finally hemin was added to the reaction buffer, and mixtures were maintained at room temperature for another 1 h, to form the hemin/G-quadruplex DNAzyme. The peroxidation reaction was initiated by the addition of H_2O_2 (100 mM, 6 μL) and TMB (12.5 mM, 3 μL) to the above solution. To stop the reaction 100 μL of 2 M H_2SO_4 was added to the solution after 15 min. Then absorbance at 450 nm of the solution was measured by using a Lambda 750 UV-vis spectrophotometer.

3 Results and discussion

Herein, we introduced a colorimetric aptasensor based on a modified ATP–Apt and a peroxidase mimicking DNAzyme as the signal transduction probe (STP). The STP sequence and two arm segments of ATP–Apt interact together *via* Watson–Crick and Hoogsteen base pairings and formed an ATP sensitive complex (THMS). In this case, the STP strand has configured the rigid structure and not able to form the G-quadruplex structure.[31,32] In the presence of ATP, the aptamer part specifically binds to it, leading to disintegration of the THMS complex. Now the free STP in combination with hemin can form the hemin/G4-quadruplex DNAzyme with peroxidase-like activity. STP–hemin complexes catalyze the oxidation reaction of TMB in the

Table 1 Oligonucleotide sequences used in this work. The boldface type is the aptamer and the underlined sequences indicate the C-rich flanked arms

Entry	Sequence
Signal transduction probe (STP)	GGGTAGGGAGGGTTGGGT
ATP–Aptamer	CCCTCCCACCTGGGGGAGTATTGCGGAGGAAGGTCCCTCCC

presence of H_2O_2 which results in an obvious color change in the reaction buffer. Scheme 1 illustrates the THMS structure and the overall mechanism of the reaction.

Interestingly, by this method, THMS complex formation can be indirectly determined by analyzing the amount of free STP in the presence of target molecules (ATP). As shown in Fig. 1A, the released STP after interaction with hemin can oxidize TMB and enhanced the absorbance compared to blank. As another blank, the mixture of ATP–Apt and hemin in the presence of TMB and H_2O_2 has an insignificant absorption below 0.1 that could be neglected.

Also, for additional validation of THMS complex formation, the interaction of ATP–Apt and STP strands was studied by electrophoresis analysis. ATP–Apt, STP and THMS solution were loaded on the agarose gel (3%) and visualized under UV after staining with ethidium bromide. Fig. 1B shows the migration pattern of the ATP–Apt, STP and THMS complex on the agarose gel in the separate lanes. As can be seen in Fig. 1b, the THMS complex appeared as a single bright band which was slightly slower than that of the ATP–Apt strand. These results indicated that the interaction between ATP–Apt and STP was specifically occurred.

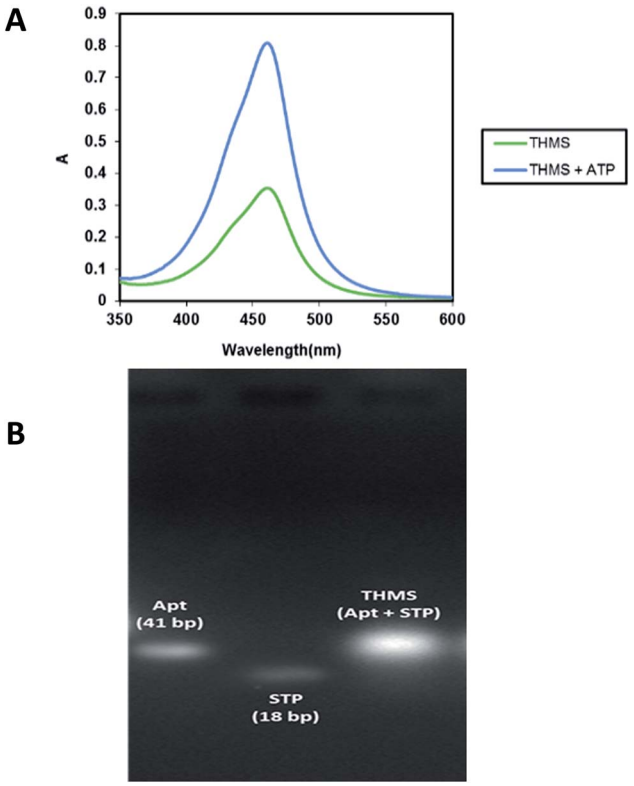

Fig. 1 (A) Absorbance of the THMS complex formed by 80 nM DNAzyme + 115 nM ATP–Apt + 88 nM hemin (orange), THMS complex (DNAzyme + ATP–Apt) + hemin (88 nM) + 130 nM ATP (blue) (λ_{max} = 450 nm). (B) The migration pattern of the ATP–Apt, STP and THMS complex on the agarose gel in the separate lanes.

3.1 Optimization of THMS complex formation

To achieve the best sensing performance, the concentration of the DNAzyme, hemin, pH and incubation time was optimized. Several different DNAzyme concentrations were added to the constant concentration of ATP–Apt. The main goal of DNAzyme optimization was to find a desirable concentration of the DNAzyme at which complex formation was fully completed and the level of free DNAzyme (noise signal) was reduced as low as possible. As is shown in Fig. 2a, the absorbance of the system increased significantly with increasing DNAzyme concentration but when the final concentration of DNAzyme reached 80 nM, the system exhibited the best sensing performance. At higher concentrations of the DNAzyme, increasing the amount of free enzyme in an environment can interfere with turnover of the aptasensor and lead to a decrease in efficiency of sensors. Therefore, the concentration of the DNAzyme at 80 nM was chosen for further ATP sensing experiments.

The objective of hemin optimization was to determine a concentration of hemin that could give us the highest

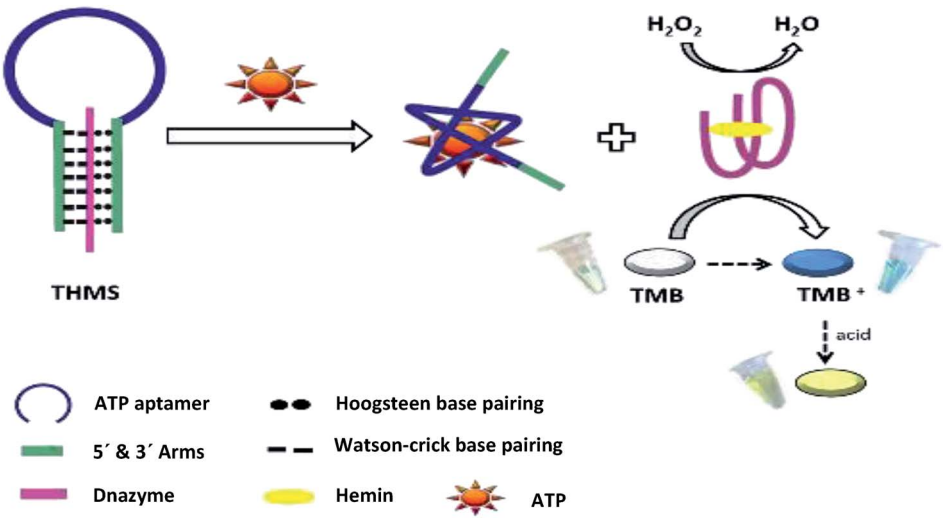

Scheme 1 Schematic description of ATP detection with the DNAzyme based aptasensor.

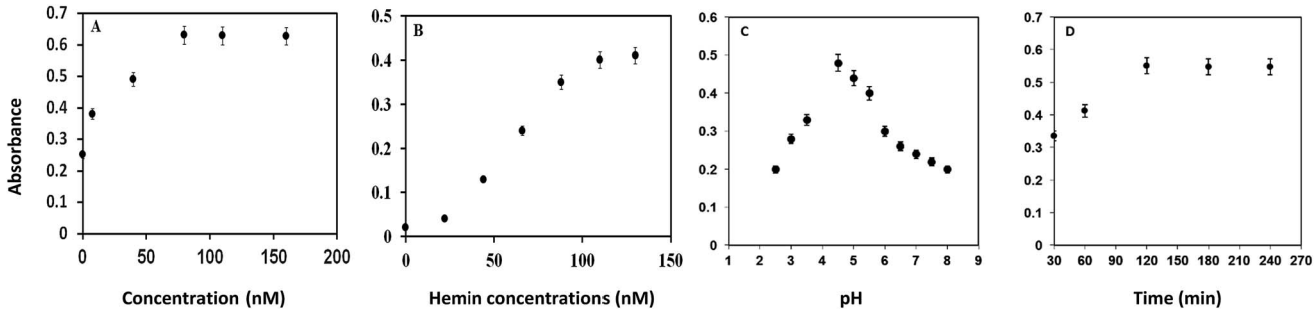

Fig. 2 (A) Histogram of the absorbance value at 450 nm for the THMS complex in the presence of different concentrations of the DNAzyme (0, 8, 40, 80, 110, and 160 nM), ATP–Apt (115 nM) and constant concentration of hemin, (B) hemin optimization; absorbance of the DNAzyme in the presence of various concentrations of hemin (0, 22, 44, 66, 88, 110, and 130 nM), (C) relative absorbance of the DNAzyme as a signal transduction probe of the THMS in the binding buffer with different pH values (2.5–8.0), and (D) effect of incubation time on the absorbance of the THMS complex.

difference in absorption between hemin and hemin-DNAzyme complexes. To obtain the optimum concentration of hemin, we investigated the peroxidase-like activity of a DNAzyme in response to different hemin concentrations (0–130 nM) in the binding buffer. Based on these results the final concentration of 88 nM hemin was the reasonable and optimized concentration for our work, because the maximum absorbance was observed at this point and the higher concentrations couldn't make significant change (Fig. 2b).

The function and formation of the THMS were also studied at different pH values (2.5–8.0). It was found that maximum formation of the THMS was achieved at pH 4.5, which showed detectable and significant difference between the blank and the target (Fig. 2c). It has been reported that the formation of Hoogsteen base pairing, formation of C-G·G^{+} triplets, and efficient interaction between the DNAzyme and the modified ATP–Apt are due to protonation of cytosine residues under weak acidic conditions.[30] Furthermore, acidic pH improves the formation and function of the hemin/G-quadruplex DNAzyme[33] and it is also reported that TMB oxidation products are more stable at acidic pH.[34]

Finally, the effect of ATP–Apt and DNAzyme incubation time on the sensor performance was investigated through the time dependency experiment. For this, ATP (40 nM) was added to the THMS complex in the reaction buffer and the absorbance was monitored at the certain time intervals. As shown in Fig. 2d, the absorbance of the DNAzyme was gradually increased and after a certain amount of time it reached a plateau. It means that the

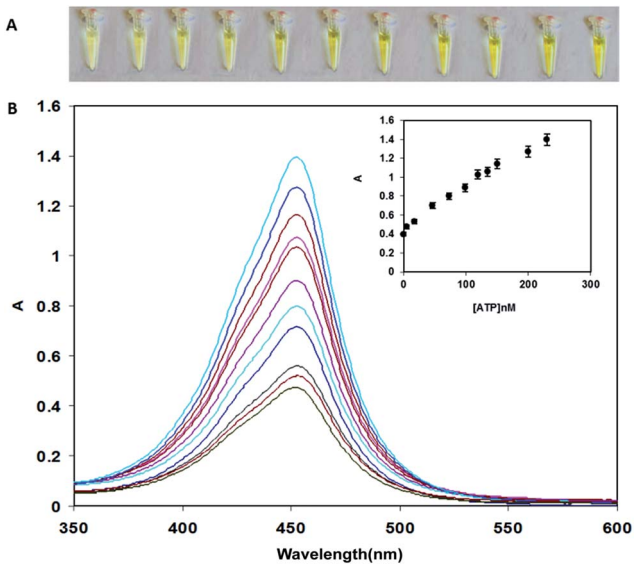

Fig. 3 (A) Relative absorbance of the THMS complex formed by the ATP–Apt (115 nM), DNAzyme (80 nM), and hemin (88 nM), in the presence of different ATP concentrations. The inset shows the logarithmic plot of fluorescence intensity *versus* target RNA concentration. (B) Color change in different concentrations of ATP.

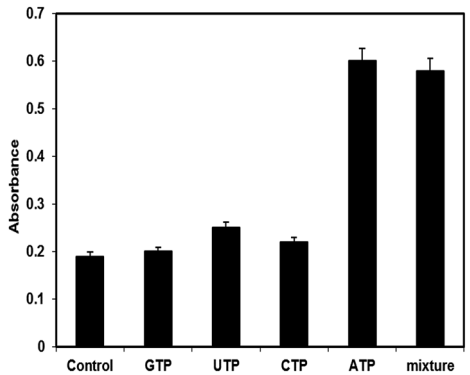

Fig. 4 Selectivity of the aptasensor by using 100 nM CTP, GTP, UTP and ATP.

Table 2 Recovery and relative standard deviation (RSD) of ATP in human serum samples

Serum samples	Added (nM)	Detected (nM)	Recovery (%)	RSD, $n = 5$ (%)
1	50	47.0	94.0	3.4
2	100	103.0	103.0	4.0
3	150	156.0	104.0	5.4
4	200	195.4	97.8	6.0

Table 3 Comparisons of other reported techniques for ATP detection

Methods	LOD	Linear range	Refs
Binding-induced collapse of DNA nano-assembly with plasmonic gold nanoparticles	24 μM	—	35
Utilizing a split aptamer target binding strategy and superior catalytic activity of graphene oxide–platinum/gold nanoparticles	0.2 nM	0–100 nM	36
Target recycling amplification based on un-modified aptamers and DNAzymes	0.33 nM	1–100 nM	37
A gold nanoparticle-based aptamer target binding readout for ATP assay	0.6 μM	4.4–32.7 μM	38
A sensitive colorimetric and fluorescent probe based on a polythiophene derivative	10 nM	10^{-6} to 5×10^{-4} M	39
Detection based on cyclic enzymatic signal amplification and a hairpin aptamer probe	25 nM	50 nM to 10 μM	40
Design an activatable hairpin probe based on a DNAzyme	67 nM	100 nM to 3 mM	41
Applying two layers of sol–gel coating binding to the end of an optical fiber probe as a sensor	1 μM	1 μM to 1.5 mM	42
Present study	2.4 nM	5–230 nM	

responsiveness and functionality of the structure of the target increased until 2 h. Thus this time was chosen as an optimized incubation time.

3.2 Sensitivity of ATP detection

To evaluate the sensitivity of the designed label-free DNAzyme aptasensor, the assay was practiced at different amounts of ATP. As shown in Fig. 3, the absorbance of the aptasensor increased significantly with increasing amount of ATP. The relationship between absorption and ATP concentration in the range of 5–230 nM is shown in the inset. The regression equation is $A = 0.0042\ C + 0.46$ in which A is the absorbance and C is the concentration of ATP in nanomolar with a correlation coefficient of 0.9854. The detection limit (defined as 3σ/slope) was determined to be 2.4 nM (where σ is the standard deviation of the blank solution) and a linear range from 5 to 230 nM under optimal conditions.

3.3 Selectivity

One of the most important characteristics of a practical sensor is selectivity. To investigate the selectivity of the designed aptasensor, effects of some ATP analogues (CTP, GTP and UTP) were analyzed under the optimal conditions. As expected, the absorbance signal upon the addition of ATP or the mixture of ATP is much higher than that of ATP analogues (Fig. 4). It was clearly shown that GTP, CTP, and UTP could not combine with the ATP–Aptamer to form the triplex and this system could not be broken and therefore, the DNAzyme could not be released and the absorbance values of the solution were not affected.

3.4 ATP detection in biological samples

In order to examine the performance of our ATP assay in real samples, the recovery test in spiked human serum was conducted. To remove macromolecules, HSA and other abundant proteins from serum, the samples were first filtered by using centrifugal filtration devices (30 K) and then diluted at different dilutions with the buffer. The results showed that the aptasensor worked well when challenged in 1% human serum. Then, in order to verify the performance of the method, certain amounts of ATP were spiked in 1% serum. As listed in Table 2, the recoveries in human serum samples were from 94.0% to 104.0% with the relative standard deviation of 3.4% to 6.0%. The results indicate that the presence of ATP in serum can be precisely detected, demonstrating the applicability of this method in complex biological samples.

The analytical performance of the proposed aptasensor was compared with other colorimetric methods reported previously in the literature, as shown in Table 3. According to Table 3, the proposed apta-sensor exhibits a wide dynamic range with a low detection limit which is better than some earlier reported methods. Therefore, the proposed aptasensor has great potential for the determination of ATP.

4 Conclusions

Herein, we proposed a new colorimetric aptasensor based on the complex of an ATP–Aptamer and a peroxidase-like DNAzyme. This fabrication is based on the principle of DNA triplex formation which was autonomously conducted *via* Watson–Crick and Hoogsteen base pairings under optimal conditions. By this simple approach the need for molecular labeling or other bioconjugation processes was diminished and a colorimetric signal discernible with the naked eye was produced. The high sensitivity and selectivity of the aptamer towards the ATP analyte and the accurate action of the DNAzyme part as a colorimetric reporter allowed us to develop a fast, simple and cheap method for ATP detection. More intriguingly, the possibility of replacement of an aptamer site with other sequences related to different targets such as miRNAs and antigens indicates the versatility of this approach and would be a fruitful area for further studies.

References

1 T. Bao, H. Shu, W. Wen, X. Zhang and S. Wang, *Anal. Chim. Acta*, 2015, **862**, 64.
2 F. Liu, J. Zhang, R. Chen, L. Chen and L. Deng, *Chem. Biodiversity*, 2011, **8**, 311.
3 J. Chen, Y. Liu, X. Ji and Z. He, *Biosens. Bioelectron.*, 2016, **83**, 221.
4 X. Li, Y. Peng, Y. Chai, R. Yuana and Y. Xiang, *Chem. Commun.*, 2016, **52**, 3673.

5 L. Jia, L. Ding, J. Tian, L. Bao, Y. Hu, H. Ju and J. S. Yu, *Nanoscale*, 2014, **7**, 15953.
6 Z. Liu, W. Zhang, W. Qi, W. Gao, S. Hanif, M. Saqib and G. Xu, *Chem. Commun.*, 2015, **51**, 4256.
7 H. Huang, Y. Tan, J. Shi, G. Liang and J. J. Zhu, *Nanoscale*, 2010, **2**, 606.
8 Z. M. Zhou, Y. Yu and Y. D. Zhao, *Analyst*, 2012, **137**, 4262.
9 L. Zhang, H. Wei, J. Li, T. Li, D. Li, Y. Li and E. Wang, *Biosens. Bioelectron.*, 2010, **25**, 1897.
10 Y. Wang, L. Bao, Z. Liu and D. W. Pang, *Anal. Chem.*, 2011, **83**, 8130.
11 R. R. Breaker and T. Sight, *Science*, 2000, **290**, 2095.
12 J. Li, W. Zheng, A. H. Kwon and Y. Lu, *Nucleic Acids Res.*, 2000, **28**, 481.
13 N. Carmi, L. A. Shultz and R. R. Breaker, *Chem. Biol.*, 1996, **3**, 1039.
14 Y. Li and R. R. Breaker, *Curr. Opin. Struct. Biol.*, 1999, **9**, 315.
15 B. Cuenoud and J. W. Szostak, *Nature*, 1995, **375**, 611.
16 Y. Li and R. R. Breaker, *Methods*, 2001, **23**, 179.
17 P. Travascio, Y. Li and D. Sen, *Chem. Biol.*, 1998, **5**, 505.
18 H. Li, Z. Wu, L. Qiu, J. Liu, C. Wang, G. Shen and R. Yu, *Biosens. Bioelectron.*, 2013, **50**, 180.
19 Y. Du, B. Li, S. Guo, Z. Zhou, M. Zhou, E. Wang and S. Dong, *Analyst*, 2011, **136**, 493.
20 J. Kosman and B. Juskowiak, *Anal. Chim. Acta*, 2011, **707**, 7.
21 Y. Geng, J. Wu, L. Shao, F. Yan and H. Ju, *Biosens. Bioelectron.*, 2014, **61**, 593.
22 P. Ling, J. Lei and H. Ju, *Biosens. Bioelectron.*, 2015, **71**, 373.
23 D. Li, B. Shlyahovsky, J. Elbaz and I. Willner, *J. Am. Chem. Soc.*, 2007, **129**, 5804.
24 J. Elbaz, B. Shlyahovsky and I. Willner, *Chem. Commun.*, 2008, 1569.
25 D. M. Kolpashchikov, *J. Am. Chem. Soc.*, 2008, **130**, 2934.
26 Y. Xiao, V. Pavlov, T. Niazov, A. Dishon, M. Kotler and I. Willner, *J. Am. Chem. Soc.*, 2004, **126**, 7430.
27 Y. L. Yuan, R. Yuan, C. Yaqin, Y. Zhuo, X. Ye, X. Gana and L. Bai, *Chem. Commun.*, 2012, **48**, 4621.
28 L. H. Tang, Y. Liu, A. Monsur, D. K. Kang, W. Zhao and J. Li, *Anal. Chem.*, 2012, **84**, 4711.
29 X. B. Zhang, R. M. Kong and Y. Lu, *Anal. Chem.*, 2011, 105.
30 J. Zheng, J. Li, Y. Jiang, J. Jin, K. Wang, R. Yang and W. Tan, *Anal. Chem.*, 2011, **83**, 6586.
31 W. Gao, L. Zhang, Y.-M. Zhang, R.-P. Liang and J.-D. Qiu, *J. Phys. Chem. C*, 2014, **118**, 14410–14417.
32 J. Zheng, A. Jiao, R. Yang, H. Li, J. Li, M. Shi, C. Ma, Y. Jiang, L. Deng and W. Tan, *J. Am. Chem. Soc.*, 2012, **134**, 19957–19960.
33 R. Li, C. Xiong, Z. Xiao and L. Ling, *Anal. Chim. Acta*, 2012, **724**, 80.
34 L. A. Marquez and H. B. Dunford, *Biochemistry*, 1997, **36**, 9349.
35 J. J. Wang, J. Lu, S. Su, J. Gao, Q. Huang, L. Wang, W. Huang and X. Zuo, *Biosens. Bioelectron.*, 2015, **65**, 171.
36 S. Zhang, K. Wang, J. Li, Z. Li and T. Sun, *RSC Adv.*, 2015, **5**, 75746.
37 X. Gong, J. Li, W. Zhou, Y. Xiang, R. Yuan and Y. Chai, *Anal. Chim. Acta*, 2014, **828**, 80.
38 J. Wang, L. Wang, X. Liu, Z. Liang, S. Song, W. Li, G. Li and C. Fan, *Adv. Mater.*, 2007, **19**, 3943.
39 C. Li, M. Numata, M. Takeuchi and S. Shinkai, *Angew. Chem., Int. Ed. Engl.*, 2005, **44**, 6371.
40 J. Li, H. E. Fu, L. J. Wu, A. X. Zheng, G. N. Chen and H. H. Yang, *Anal. Chem.*, 2012, **84**, 5309.
41 W. J. Chen, Y. Hu, J. Li, Y. Li, J. Bai, J. Zheng and R. Yang, *Anal. Methods*, 2014, **6**, 3219.
42 C. Wang, C. Y. Huang and W. C. Lin, *Biosens. Bioelectron.*, 2013, **43**, 355.